Gravity anomalies of the Northern Hawaiian Islands: Implications on the shield evolutions of Kauai and Niihau

Ashton F. Flinders,[1] Garrett Ito,[1] and Michael O. Garcia[1]

Received 13 August 2009; revised 29 January 2010; accepted 16 March 2010; published 31 August 2010.

[1] New land and marine gravity data reveal two positive residual gravity anomalies in the Northern Hawaiian Islands: one over Kaua'i, the other between the islands of Kaua'i and Ni'ihau. These gravitational highs are similar in size and magnitude to those of other Hawaiian volcanoes, indicating local zones of high-density crust, attributed to olivine cumulates in solidified magma reservoirs. The residual gravity high over Kaua'i is located in the Līhu'e Basin, offset 8-12 km east of Kaua'i's geologically mapped caldera. This offset suggests that the mapped caldera is a collapsed feature later filled in with lava and not the long-term center of Kaua'i shield volcanism. A second residual gravity high, in the submarine channel between Kaua'i and Ni'ihau, marks the volcanic center of the Ni'ihau shield volcano. This second residual gravity anomaly implies that Ni'ihau's eastern boundary extended ~20 km east of its present location. Through inversion, the residual gravity anomalies were modeled as being produced by two solidified magma reservoirs with average densities of 3100 kg/m^3 and volumes between 2470 and 2540 km^3. Considering the locations and sizes of the residual gravity anomalies/magma reservoirs, the extent of the two islands' paleoshorelines and potassium-argon dating of shield-stage lavas, we conclude that the two islands were not connected subaerially during their respective shield stages and that Ni'ihau's topographic summit was removed by an eastern flank collapse between 4.3 and 5.6 Ma. Continued constructional volcanism on western Kaua'i likely covered much of the submerged remains of eastern Ni'ihau.

Citation: Flinders, A. F., G. Ito, and M. O. Garcia (2010), Gravity anomalies of the Northern Hawaiian Islands: Implications on the shield evolutions of Kauai and Niihau, *J. Geophys. Res.*, *115*, B08412, doi:10.1029/2009JB006877.

1. Introduction

[2] Hotspot island volcanoes are associated with distinct positive gravity anomalies, typically located over their volcanic summits and rift zones [*Krivoy and Eaton*, 1961; *Kinoshita et al.*, 1963; *Clouard et al.*, 2000; *Kauahikaua et al.*, 2000]. Positive gravity anomalies suggest dense structures in the crust [*Strange et al.*, 1965], commonly attributed to crystallized olivine cumulates in the volcano's central magmatic reservoir [*Clague*, 1987; *Clague and Denlinger*, 1994]. These reservoirs represent regions of concentrated high-density cumulates and solidified intrusions, collected over hundreds of thousands of years [*Ryan*, 1988]. Past studies on the island of Hawai'i [*Kauahikaua et al.*, 2000] and in French Polynesia [*Clouard et al.*, 2000] have used gravity surveys to estimate the size and depth of these magma reservoirs and to identify the island's volcanic centers. Inversion of the residual gravity field allows for delineation of the 3-D density structure beneath these volcanic islands, providing constraints on the geometry and density of the magma reservoirs [*Kauahikaua et al.*, 2000]. Reconnaissance studies of the islands of Kaua'i and Ni'ihau, in the Hawaiian Island Chain, identified distinct gravity highs displaced from the topographic summits of the islands [*Krivoy*, 1965; *Krivoy et al.*, 1965]. These islands are the oldest islands (>5 Ma) in the main portion of the Hawaiian Island Chain [*McDougall*, 1979; *Sherrod et al.*, 2007]. Extensive mass wasting, erosion, and subsidence have obscured the extent, shape, and centers of their original shield volcanoes.

[3] Kaua'i has classically been interpreted as the eroded remnant of a single shield volcano [*Dana*, 1890; *Clague*, 1990], the Waimea shield [*Macdonald et al.*, 1960], centered in a region of northwest Kaua'i defined by the Olokele volcanic member [*Stearns*, 1946]. The Olokele Volcanics comprise a central plateau of thick, near horizontal, primarily tholeiitic lava flows, delineating what has been inferred to be the summit caldera of the original shield volcano, Figure 1 [*Macdonald et al.*, 1960]. A previous reconnaissance gravity survey of Kaua'i identified a Bouguer gravity high (340 mGal) in the northern portion of the Līhu'e Basin, a topographic depression forming the eastern side of the island (Figure 1), approximately 16 km east of the geologically mapped caldera [*Krivoy et al.*, 1965]. No explanation has been given for the offset of the gravity high from the caldera. Data coverage is incomplete, and the need for a more extensive survey was emphasized by *Krivoy et al.* [1965]. A subsequent paleomagnetic and geochemical study suggested

[1]Department of Geology and Geophysics, University of Hawai'i, Honolulu, Hawaii, USA.

0148-0227/10/2009JB006877

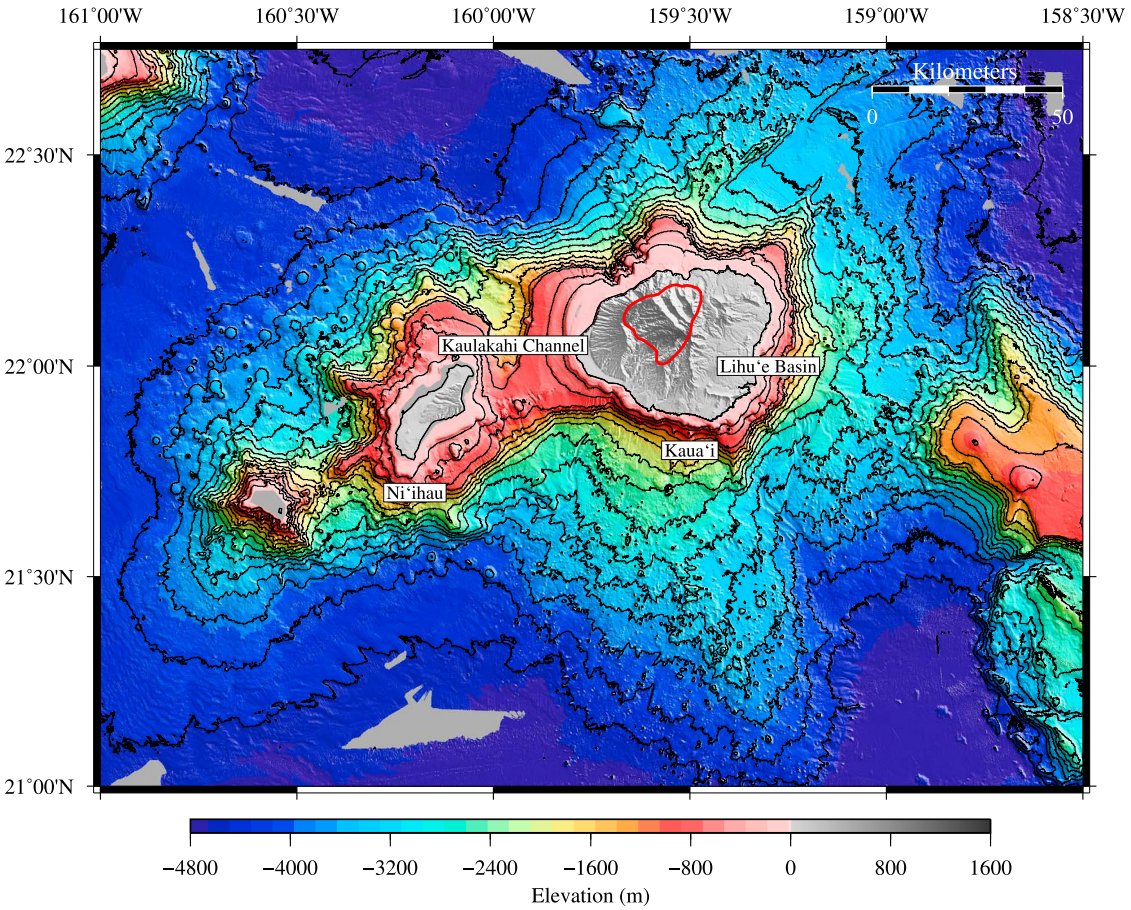

Figure 1. Digital elevation map of the islands of Kaua'i and Ni'ihau with bathymetry of surrounding seafloor (bathymetric contour interval 300 m). The red line on Kaua'i outlines the boundaries of the inferred Waimea shield caldera; the Olokele volcanic member [*Macdonald et al.*, 1960]. Bathymetry was obtained from the Main Hawaiian Islands Multibeam Synthesis (http://www.soest.hawaii.edu/HMRG), and subaerial topography from the United States Geological Survey (USGS) (http://seamless.usgs.gov). Solid gray areas indicate regions where no bathymetry data are available.

that Kaua'i is composed of not one but multiple shield volcanoes, each having a distinct magma supply system [*Holcomb et al.*, 1997], further warranting a more detailed examination of the island.

[4] Ni'ihau, ~28 km southwest of Kaua'i, is the eroded remnant of a shield volcano the formation of which preceded and partially overlapped in time with the growth of Kaua'i [*Stearns*, 1947; *McDougall*, 1979; *Sherrod et al.*, 2007]. Hundreds of dikes are exposed on an eastern cliff margin [*Stearns*, 1947], and a reconnaissance gravity survey revealed a linear Bouguer gravity high trending northeast, parallel to the channel running between the two islands (Kaulakahi Channel, Figure 1) [*Krivoy*, 1965]. The local gravity field was inferred to support the geologic mapping of *Stearns* [1947], which placed the center of Ni'ihau volcanism ~3 km east of the island's eastern cliff margin [*Krivoy*, 1965].

[5] Submarine terraces surround the Kaulakahi Channel, between Kaua'i and Ni'ihau, and extend discontinuously around both islands (Figure 1). These terraces vary in depth between 800 and 1400 m below sea level (bsl) and are thought to delineate the original maximum extent of the shield-stage paleoshorelines before they were submerged by island subsidence [*Mark and Moore*, 1987]. Thus, the locations of the paleoshorelines constrain the dimensions of the shield-stage islands. By combining paleoshorelines with gravity data, we can infer where the original volcanic summits were in relation to the shield-stage island boundaries.

[6] We performed a new gravity survey on the island of Kaua'i, with the goal of completing the reconnaissance survey of *Krivoy et al.* [1965]. In addition, a new offshore gravity and bathymetry survey around both islands was undertaken onboard the University of Hawai'i's *R/V Kilo Moana* (cruise KM0718). We integrated these data with a previous survey of Ni'ihau [*Krivoy*, 1965] and three additional new marine gravity data sets to identify offshore gravity highs and characterize the regional gravity field. We present a model for the geological evolution of the shield stages of both islands, based on the locations and sizes of residual gravity highs, the inverted crustal density structure, the extent of paleoshorelines, and potassium-argon dating of shield-stage lavas.

2. Data Collection and Reduction

2.1. Initial Collection and Corrections

[7] Between May and September 2008, 315 measurements were collected on the island of Kaua'i using a LaCoste and

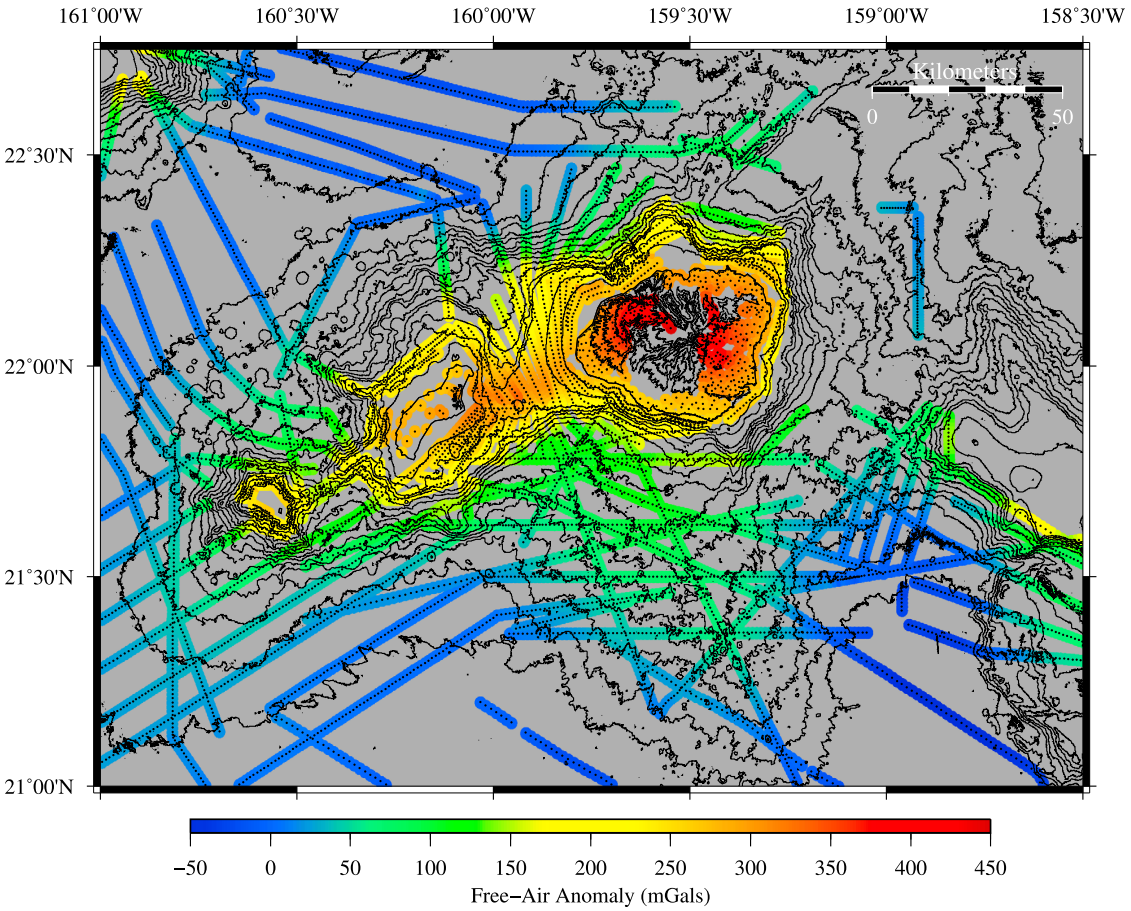

Figure 2. Free-air anomaly (FAA) map of Kaua'i, Ni'ihau, and the surrounding submarine area. The data set is composed of a new gravity survey performed on Kaua'i, a previous survey of Ni'ihau [*Krivoy*, 1965], and four marine-based gravity surveys (see text for details). The marine data consisted of 149 tracklines, 77 of which crossed more than one different trackline (a total of 195 crossings). Solid black dots show locations where the gravity field was measured. Both the Kaulakahi Channel and the Līhu'e Basin (see Figure 1) show anomalously high FAA gravity compared to surrounding regions of similar elevation. For visualization, we gridded the multiple data sets using a "nearest-neighbor" algorithm [*Wessel and Smith*, 1991]. Bathymetric contour interval is 300 m. Gray areas indicate regions with no gravity data.

Romberg G gravimeter. Tidal effects in the data were removed by using a second LaCoste and Romberg G gravimeter to record tidal variations (<0.3 mGal) in the gravity at our base station location. These daily fluctuations were eliminated from the field data, and a linear correction was applied to account for instrumental drift with time. The average drift correction between base station reoccupations (~12 h) was 0.1 mGal, providing an estimate of the instrumental uncertainty. The 315 new measurements were merged with 22 from a past survey of the island of Ni'ihau performed by *Krivoy* [1965]. The original Kaua'i reconnaissance survey data [*Krivoy et al.*, 1965] were not incorporated into this study because our new data covered a more extensive area at a finer spatial resolution, were more precisely located using high-precision GPS, and were of comparable values.

[8] The subaerial data were merged with our new marine survey, collected in September of 2007 (KM0718), and three additional marine-based gravity data sets: two collected recently onboard the *R/V Kilo Moana* (KM0326, KM0512) and the third from the GLORIA surveys [*Ponce et al.*, 1994]. To eliminate unreliable data, we manually removed chaotic peaks, high-frequency noise (typically due to changes in survey speed or course), and data collected during ship turns. To improve the internal consistency of the shipboard data (5953 points), we corrected for discrepancies in measurements between crossing survey lines. Corrections were calculated by breaking the tracklines into straight segments, producing 149 separate lines and 195 different crossings. A least squares approach was used to minimize crossover errors between overlapping tracklines for all cruise data, and appropriate constant corrections were then applied, specific to each trackline, to correct for crossover errors [*Prince and Forsyth*, 1984]. The standard deviation of the corrected crossings was 4 mGal and provided a constraint on the uncertainty of the marine data.

2.2. Free-Air Gravity Anomaly

[9] Free-air anomalies (FAAs) were produced by removing the effects of the World Geodectic System 1984 (WGS84) reference ellipsoid from the raw gravity data. This was followed by correcting all land-based measurements for station elevation, obtained from high-precision GPS. Variation of

Table 1. Flexural Correction Parameters

Parameter	Value
ρ_w	1000 kg/m^3
ρ_a	2000–3250 kg/m^3
ρ_b	2000–3250 kg/m^3
ρ_m	3300 kg/m^3
z_m	15 km
D	$\frac{ET_e^3}{12(1-\nu^2)}$
ν	0.25
T_e	15–45 km
E	8.0×10^{10} N/m
g	9.8 m/s^2
γ	6.67×10^{-11} Nm^2/kg^2

the geoid over Kaua'i, relative to the WGS84 reference ellipsoid, is at maximum 3 m and was removed from GPS elevations using the GEOID09 model: available from the National Geodetic Survey (http://www.ngs.noaa.gov). Kaua'i FAA data were shifted by −10 mGal relative to the marine data in order to ensure a smooth trend between coastal land gravity and near offshore gravity.

[10] For visualization, the multiple data sets were merged using a "nearest neighbor" gridding algorithm that computed the value of each node of a geographic grid based on a weighted mean of the nearest data points [*Wessel and Smith*, 1991]. The regional data, gridded at an interval of 0.005°, are shown in Figure 2. Both the Kaulakahi Channel (between Kaua'i and Ni'ihau) and the Līhu'e Basin on eastern Kaua'i show anomalously high FAA gravity when compared to surrounding regions of similar elevation (Figure 2).

2.3. Complete Bouguer Anomaly

[11] Complete Bouguer anomalies were calculated using a two-part terrain correction: one for bathymetry and the other for subaerial topography. The bathymetric terrain correction accounted for the gravity contribution resulting from replacing the surrounding ocean water (density of ρ_w) with submarine crust (density of ρ_b) using an infill density of $\rho_b - \rho_w$, (Table 1). The topographic terrain correction accounted for the gravity contribution of subaerial mass surrounding the observation locations, using a crustal density of ρ_a (Table 1). The topographic terrain correction on Kaua'i was calculated using a 0.001° spaced digital elevation model (DEM) obtained from the United States Geological Survey (USGS) (http://seamless.usgs.gov). All other terrain corrections (surrounding bathymetry and Ni'ihau topography) were performed using a regional DEM (250 × 250 km) gridded at 0.005° provided by the Main Hawaiian Islands Multibeam Synthesis (MHIMS) (http://www.soest.hawaii.edu/HMRG). The regional DEM was divided at mean sea level into two gridded data sets: one containing bathymetry and the other topography. Each grid element defined the top surface of a 3-D prism, and the gravitational attraction of all prisms [*Blakely*, 1996] within 0.2° of individual gravity measurements was removed from the free-air anomaly to produce a map of the complete Bouguer anomaly (Figure 3).

[12] The complete Bouguer anomaly map (Figure 3) was calculated using values of ρ_b = 2700 kg/m^3 and ρ_a = 2400 kg/m^3, which minimized variability within the anomaly and agreed with geological constraints (see section 3.1). The regions of anomalously high gravity in the Kaulakahi Channel and the Līhu'e Basin are more distinct after terrain effects were removed. A long wavelength decrease in Bouguer gravity west-to-east was observed south of the islands (Figure 3). This long wavelength signal is caused by flexure of the oceanic lithosphere.

2.4. Residual Gravity Anomaly

[13] Past studies of the gravity field of the Hawaiian Islands have shown that the islands act as regionally supported loads on the flexing oceanic lithosphere [*Walcott*, 1970]. A thin elastic plate approximation [*Watts and Cochran*, 1974] was used to compute the variation in gravity resulting from flexural deformation of the lithosphere caused by loading from Kaua'i, Ni'ihau, and the surrounding islands. The flexural calculation was performed using a larger regional DEM (1200 × 1200 km) spanning the main Hawaiian Islands and extending out to Necker island, approximately 600 km east of Kaua'i. Where available, this DEM included data from the MHIMS (http://www.soest.hawaii.edu/HMRG) and the USGS (http://seamless.usgs.gov). For bathymetry outside of this region, seafloor topography derived from satellite altimetry, correlated with ship depth soundings, were used [*Smith and Sandwell*, 1997].

[14] The larger regional DEM was gridded at 2 km intervals, separated into topographic and bathymetric loads, and then padded by reflecting it about its boundaries to avoid edge effects. The Fourier transformed deflection (W) of an ideal elastic plate of an effective thickness (T_e), beneath Fourier transformed topography (H) and bathymetry (B) [*Turcotte and Schubert*, 2002; *Parker*, 1973] was calculated according to

$$W_B(k_x, k_y) = -\left(\frac{\rho_b - \rho_w}{\rho_m - \rho_b}\right)\left[1 + \frac{(2\pi k)^4 D}{(\rho_m - \rho_b)g}\right]^{-1} B(k_x, k_y) \quad (1)$$

$$W_H(k_x, k_y) = -\left(\frac{\rho_a}{\rho_m - \rho_b}\right)\left[1 + \frac{(2\pi k)^4 D}{(\rho_m - \rho_b)g}\right]^{-1} H(k_x, k_y), \quad (2)$$

where k_x and k_y are horizontal wave numbers, k is their Euclidean norm, D is the flexural rigidity of the plate, g is the acceleration due to gravity, and ρ_m and ρ_w are densities of the mantle and water, respectively. Again, two values for the crustal density were considered: ρ_a is the density of the crust above sea level, and ρ_b is the density of the crust below sea level, which also defines the contrast at the crust-mantle interface (Moho). The gravity field resulting from the deflected Moho is described using the method of *Parker* [1973],

$$\Delta G(k_x, k_y) = 2\pi\gamma(\rho_m - \rho_b)e^{-2\pi k z_m}\left[W_B(k_x, k_y) + W_H(k_x, k_y)\right], \quad (3)$$

where z_m = 15 km is the average depth to the Moho, estimated from seismic reflection beneath O'ahu, extrapolated out to Kaua'i [*Watts and ten Brink*, 1989].

[15] The flexural gravity contribution was removed from the complete Bouguer anomaly data to produce isostatic anomalies. Crustal densities and effective elastic plate thicknesses used in the flexural model are given in Table 1. The mean of the isostatic anomaly field was removed to produce a residual anomaly map as shown in Figures 4a and 5, using values of ρ_b = 2700 kg/m^3, ρ_a = 2400 kg/m^3, and T_e = 35 km. An elastic plate thickness of 35 km minimizes

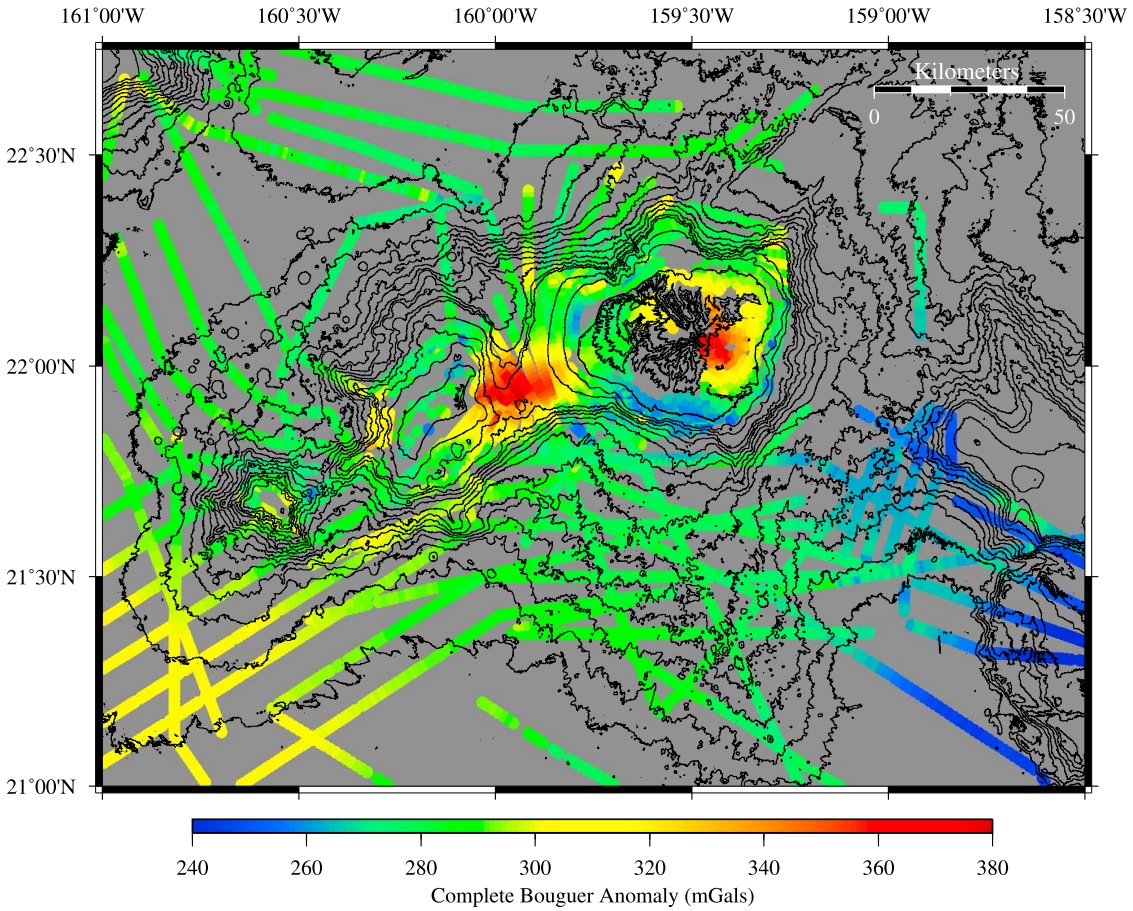

Figure 3. Complete Bouguer anomaly map of Kaua'i, Ni'ihau, and the surrounding submarine area. The regions of anomalously high FAA gravity, over the Kaulakahi Channel and the Līhu'e Basin, are distinct after removal of terrain effects. A long wavelength decrease (~45 mGal) in gravity from west-to-east is evident south of the islands, which is probably caused by flexure of the oceanic lithosphere. Bathymetric contour interval is 300 m. Gray areas indicate regions with no gravity data.

the variability within the residual gravity anomaly and agrees with values found by previous studies (see section 3.1). The main effect of the flexural correction was to remove the long wavelength west-to-east gradient in the complete Bouguer anomaly. The amplitude of the short wavelength highs over the Līhu'e Basin on Kaua'i and over the Kaulakahi Channel was largely unchanged. The residual gravity high over the Kaulakahi Channel is approximately 20 × 30 km (NW by NE, respectively) with maximum amplitude of 107 mGal. The residual gravity high over the Līhu'e Basin is approximately 20 × 20 km, with a maximum amplitude of 95 mGal.

3. Analysis

3.1. Residual Analysis and Density Determination

[16] The values for the submarine (ρ_b) and subaerial (ρ_a) crustal densities and the elastic plate thickness (T_e) used in the previously described data reduction minimized the variation, or standard deviation, of the residual gravity over our study region. These values were found by varying the crustal densities (ρ_b, ρ_a) between 2000 and 3250 kg/m^3 and the elastic plate thickness between 15 and 45 km. Analysis showed a minimum standard deviation of 16 ± 1 mGal for $\rho_b = \rho_a =$ 2700–2900 kg/m^3 and $T_e = 35 \pm 10$ km. Thus, for our reference density structure, we assume a mean submarine density of ρ_b = 2700 kg/m^3. This density minimizes the variability within our residual gravity anomaly and falls between a density of 2600 kg/m^3 as used in the gravity study of the island of Hawai'i by *Kauahikaua et al.* [2000] and a computed X-ray fluorescence (XRF) whole rock density [*Bottinga and Weill*, 1970] of 2830 kg/m^3, calculated from the mean composition of 27 Kaua'i shield-stage lavas [*Mukhopadhyay et al.*, 2003]. As expected, the analysis was largely insensitive to the chosen subaerial density, as the bulk of the islands mass lies below sea level. Therefore, for the subaerial density, we chose a value of ρ_a = 2400 kg/m^3. This reflects the calculated whole rock XRF rock data density with 15% vesicularity [*Cashman and Kauahikaua*, 1997] and agrees with densities derived from seismic *P* wave speeds for subaerial and shallow-water pillow flows for Hawaiian basalts [*Zucca et al.*, 1982].

[17] An elastic plate thickness of T_e = 35 km was employed; however, the flexure correction primarily influenced variations at wavelengths longer than those of the local highs that dominate the variability within the residual gravity anomaly. The insensitivity of these local highs to T_e is reflected by the large range of T_e (i.e., ±10 km) that minimizes the residual anomaly. A value of 35 km is within the range of 25–40 km

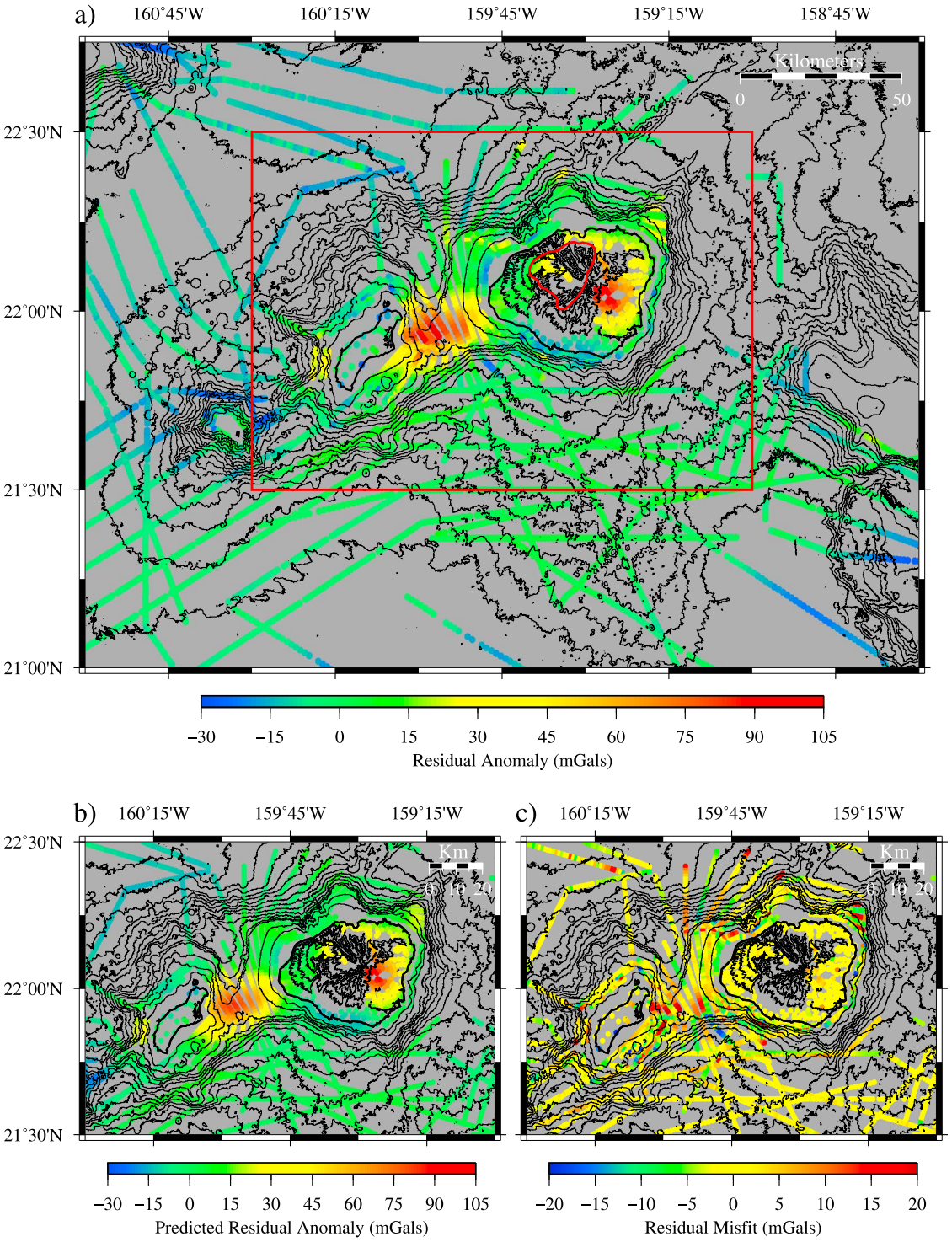

Figure 4. (a) Residual gravity anomaly map of Kaua'i, Ni'ihau, and the surrounding submarine area. The red box marks the region used in the inversion. The red line on Kaua'i outlines the boundaries of the inferred Waimea shield caldera, the Olokele volcanic member [*Macdonald et al.*, 1960]. (b) Residual anomaly predicted by forward modeling the density structure found from inversion (Figure 8). (c) Residual misfit (observed minus predicted residual gravity anomaly). Bathymetric contour interval is 300 m. Gray areas indicate regions with no gravity data.

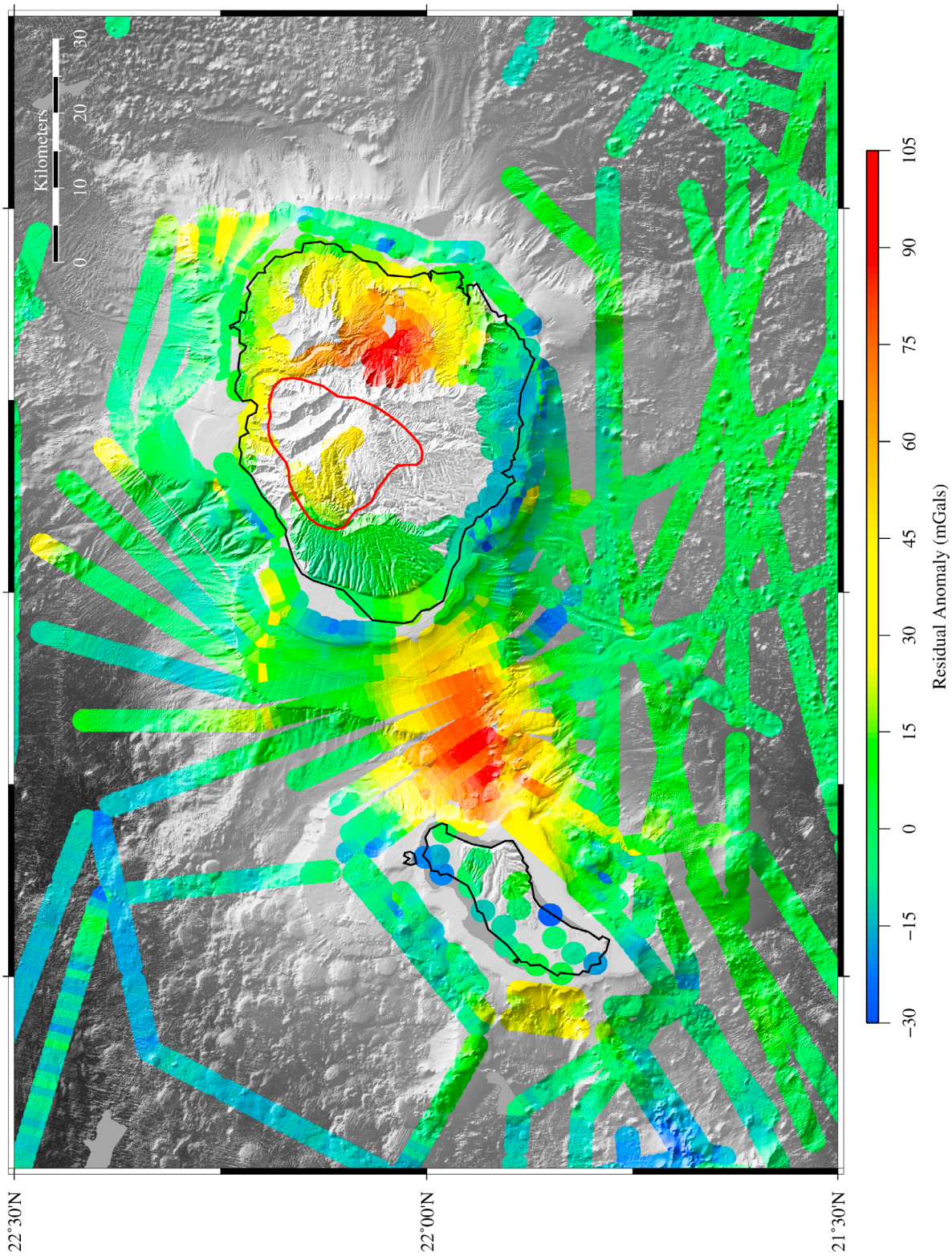

Figure 5. Detailed residual gravity anomaly map (color overlay) using $\rho_b = 2700$ kg/m^3, $\rho_a = 2400$ kg/m^3, and $T_e = 35$ km, draped over gray shaded digital elevation, illuminated from the northeast. The red line on Kaua'i outlines the boundaries of the inferred Waimea shield caldera; the Olokele volcanic member [*Macdonald et al.*, 1960]. Gray areas indicate regions with no gravity data.

found by previous studies [*McNutt and Shure*, 1986; *Watts and ten Brink*, 1989; *Wessel*, 1993; *Wessel and Keating*, 1994]. The residual anomaly shown in Figure 4a and Figure 5 was produced from the above crustal densities and elastic plate thickness. These densities define a reference structure from which density variations are determined using the inversion method discussed in section 3.3.

3.2. Rejuvenated Volcanics Density Model

[18] Rejuvenated lavas, are among the most dense of Hawaiian lavas [*Macdonald et al.*, 1983], and therefore, we explored their potential influence on the high residual gravity over Kaua'i. Rejuvenated-alkalic lavas on eastern Kaua'i (Kōloa Volcanics [*Stearns*, 1946]) have whole rock XRF densities of up to 2990 kg/m^3 [*Maaloe et al.*, 1992]. These lavas mantle eastern Kaua'i to depths of at least 300 m bsl [*Reiners et al.*, 1999; *Garcia et al.*, 2010]. To test the effects of these high-density lavas on the gravity contribution, we defined a region in the Līhu'e Basin bound by the subaerial mapping of the Kōloa Volcanics [*Macdonald et al.*, 1960], extending from the surface elevation to the maximum depth observed in well logs [*Reiners et al.*, 1999; *Garcia et al.*, 2010]. A density model for all mass within this region was created and incorporated into our terrain correction. Calculations revealed that explaining the residual gravity high over the Līhu'e Basin required a geologically unreasonable density of the Kōloa Volcanics of at least 7000 kg/m^3. A density of 2990 kg/m^3 for the Kōloa Volcanics resulted in only a small (<3 mGal) reduction of the residual high. The contribution of the rejuvenated lavas to the residual gravity was statistically insignificant. Thus, we used a uniform subaerial density of 2400 kg/m^3 in our subsequent gravity inversion.

3.3. Three-Dimensional Inversion

[19] The residual gravity data were inverted, and 3-D models of subsurface density contrast were generated using the GRAV3D program library [*GRAV3D*, 2007]. The residual anomaly data set consisted of 2921 measurements and was bound to the region shown in Figures 4a and 5. GRAV3D models the subsurface volume by dividing the region of interest into a set of 3-D boxes, each with a constant density contrast, bound by an orthogonal mesh. The density distribution is found by solving the inversion as an optimization problem with the goals of minimizing a model objective function (a combination of the model norm and misfit) and generating synthetic data that fall within the statistical misfit of the observations [*Li and Oldenburg*, 1998]. For details on inversion methodology, refer to Appendix A.

[20] The uncertainty of the residual anomalies (σ_i) determines how precisely the inversion reproduces the observed data and is therefore the most important factor in determining the type of density model produced. Large uncertainties produce poorly constrained models (highly variable), whereas small uncertainties tend to concentrate density variations on the upper surface of the model space, which are typically too short of wavelength and too high in amplitude to be geologically reasonable. The uncertainty for marine observations was dominated by the average crossover error (4 mGal) at survey trackline crossings. Land-based measurement uncertainties were dominated by terrain correction uncertainties. These uncertainties were estimated by finding the difference (Δh) between the elevation at our observation point, measured by high-precision GPS measurements, and the elevation given by sampling the local DEM. The uncertainty in the residual gravity was therefore caused by an uncertainty in the terrain correction at each observation location, equal to the gravity contribution from an infinite (Bouguer) slab of thickness Δh. The uncertainties of measurements made on Kaua'i were calculated using the 0.001° local DEM, whereas those on Ni'ihau were calculated using the 0.005° regional DEM. The mean uncertainty in the residual anomaly on Kaua'i was 1.9 ± 0.7 mGal and on Ni'ihau was 2.9 ± 3.6 mGal. Additionally, 1.0 mGal was added to all residual uncertainties to account for the effects of terrain more than 0.2° away from individual gravity measurements, and 1% of the residual value was added to account for undetermined errors.

[21] The model space consisted of 156 × 112 × 28 prismatic cells in east-west, north-south, and up-down, respectively, resulting in 489,216 finite elements. The cells spanned 1 km in east-west/north-south and had a thickness that varied from 500 m for cells above 10 km bsl, to 1 km for all deeper cells. The top of the model space was bound by elevations from the 0.005° regional DEM, regridded to 1 km. The bottom of the model space was bound by our assumed average depth to the Moho of 15 km. The inversion problem was solved iteratively and solutions were bound to yield densities below that of olivine, 3300 kg/m^3. Iterations ceased when the cumulative normalized data-misfit ϕ_d was within 1% of the total number of observation points (equation A3). Comparison between a forward model of the best-fit inversion model (Figure 4b) and the observed residual gravity anomaly resulted in a mean misfit of 3 ± 4 mGal (Figure 4c).

[22] The inversion produced two distinct bodies with densities greater than the reference density of 2700 kg/m^3 (Figure 6), both extending to the imposed base of the model space. The first of the anomalous bodies, located under the Kaulakahi Channel, has a roof depth between 3.5 and 4.5 km bsl and a total volume of 2540 km^3 for ρ_{avg} = 3100 kg/m^3. Approximately half of this volume (1200 km^3) consists of material with a density greater than 3100 kg/m^3 (Table 2). The second anomalous body, located under the Līhu'e Basin, has a roof depth between 2 and 3 km bsl and is inclined to the south-east with respect to the base of the anomaly. This density anomaly has a total volume of 2470 km^3 for ρ_{avg} = 3100 kg/m^3, with 1130 km^3 consisting of material with a density greater than 3100 kg/m^3 (Table 2).

3.4. Paleoshoreline Analysis

[23] Identifying the paleoshorelines around the islands of Kaua'i and Ni'ihau allowed us to reconstruct the maximum lateral extents of each islands' original subaerial shield volcano [e.g., *Mark and Moore*, 1987]. These reconstructed island boundaries should enclose the gravity anomalies and therefore the inferred magma reservoirs. Paleoshorelines were determined by identifying submarine topographic slope breaks in the bathymetry around both Kaua'i and Ni'ihau (Figures 7 and 8). These slope breaks delineate the change between lavas erupted subaerially, which cooled slowly, forming low slope angles, and those erupted underwater, which cooled rapidly forming higher slope angles [e.g., *Moore*, 1987]. Reef growth contributes minimally to the slope change at this subaerial-submarine transition zone

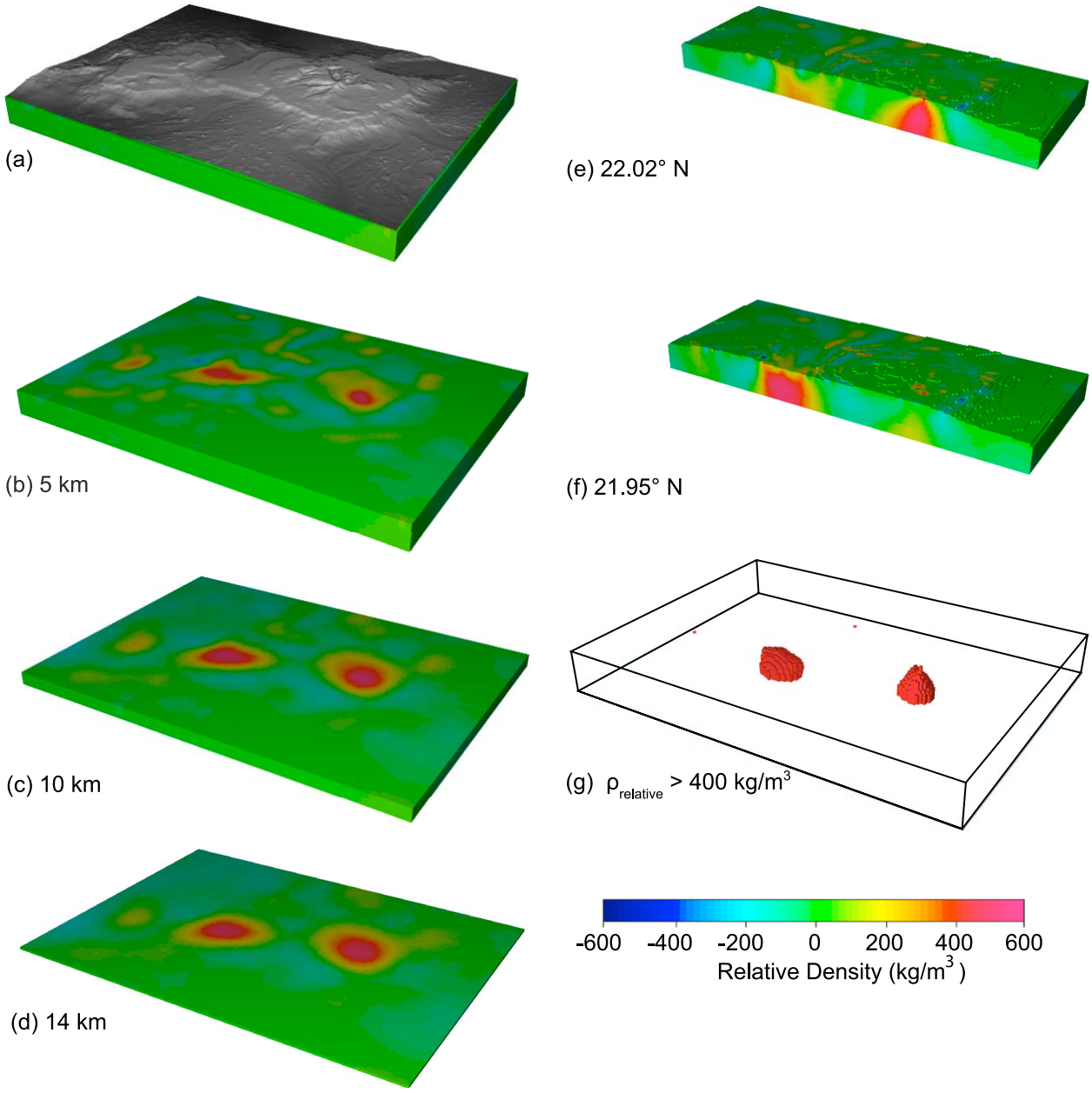

Figure 6. Density structure produced by inversion of the residual gravity anomaly. Density variations are relative to 2700 kg/m^3 (submarine density used in reducing the FAA to the residual anomaly). Variations are bound in the inversion to be <600 kg/m^3 yielding absolute density <3300 kg/m^3, the density of olivine. (a) Overlay of gray shaded digital elevation. Horizontal slices though the model shown with top surfaces at (b) 5 km, (c) 10 km, (d) 14 km. (e) East-west slice through the Kaua'i anomaly at 22.02°N and (f) the Ni'ihau anomaly at 21.95°N. (g) Isosurface showing densities greater than 3100 kg/m^3.

Table 2. Characteristics of Magma Reservoirs

	Volcano Volume[a] (×10^3 km^3)	Caldera Diameter[b] (km)	Magma Reservoir ($\rho \geq 3100$ kg/m^3)		Magma Reservoir[c] ($\rho_{avg} = 3100$ kg/m^3)	
			Volume (km^3)	Roof Depth (km)	Volume (km^3)	Roof Depth (km)
Niihau	25.3	Unknown	1200	4.5	2540	3.5
Kauai	69.0	19 × 16	1130	3.0	2470	2.0

[a]Volcano volumes from "initial" volumes of *Robinson and Eakins* [2006].
[b]Caldera dimensions from *Macdonald et al.* [1960].
[c]ρ_{avg} is calculated from the anomalous mass of each density contribution and the total volume.

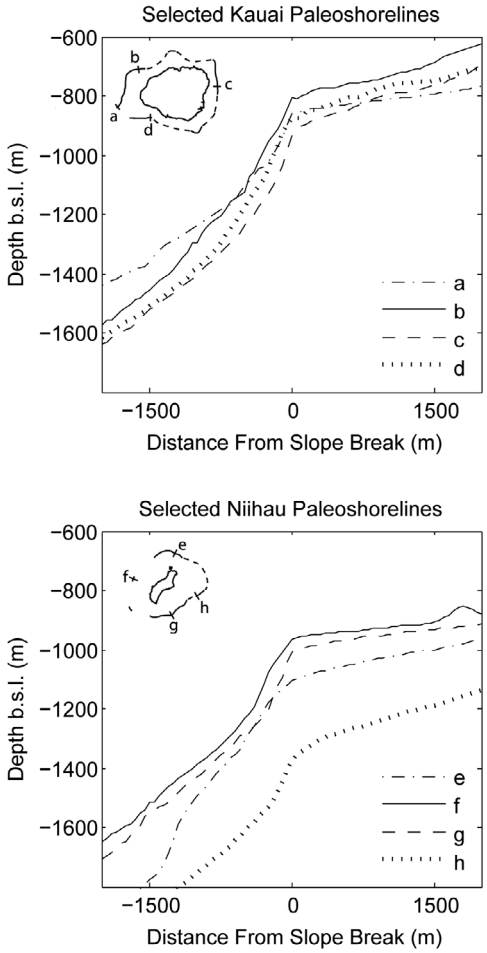

Figure 7. Selected paleoshorelines profiles of Kaua'i and Ni'ihau. Paleoshorelines were determined by identifying submarine topographic slope breaks in the bathymetry around the islands of Kaua'i and Ni'ihau. Fourteen locations showing slope breaks were identified around Kauai and 10 around Niihau, 8 of which are shown here.

[*Mark and Moore*, 1987]. The slope breaks form an identifiable paleoshoreline, assuming they were maintained when the vertical growth of the shield volcano outpaced subsidence, caused by depression of the oceanic lithosphere [*Walcott*, 1970]. As the shield building stage waned, vertical growth of the island no longer kept pace with subsidence, and the former shoreline is submerged. Thus, the deepest slope breaks delineate the original maximum extent of the shoreline before shield building declined and subsidence submerged this feature [*Mark and Moore*, 1987]. Other shallower slope breaks may form, reflecting the interplay between volcanic growth and subsidence, as well as glacially induced sea level changes [e.g., *Stearns*, 1946].

[24] The bathymetric data used for identifying slope break features around Kaua'i and Ni'ihau included swath bathymetry obtained during our KM0718 cruise and data from the MHIMS (http://www.soest.hawaii.edu/HMRG), all gridded at 50 m spacing. The paleoshoreline slope breaks were determined by finding the depths at which the bathymetry profiles, taken perpendicular to the strike of the submerged terraces surrounding the islands, changed from 4° to 9° to >15° as described by *Schmidt and Schmincke* [2000]. Slope angles were averaged over distances of 2 km seaward and shoreward of the identified slope breaks (Figure 7). Fourteen areas showing slope breaks were identified around Kaua'i and 10 around Ni'ihau (Figure 8).

[25] The depth of Kaua'i's paleoshoreline increases from 850 m bsl west of the island to 1000 m bsl east of the island (Figures 7 and 8). The mean slope of Kaua'i's bathymetry profiles above the slope break is 4° ± 2°. Below the slope break, the slope is 17° ± 3°. A plane was fit to the paleoshoreline depths to reconstruct the original terrace formed by the Kaua'i shield-stage shoreline, here called the N terrace (after the Nāpali Volcanics, the shield building lavas of Kaua'i [*Macdonald et al.*, 1960]). The N terrace dips 0.14° in the direction of O'ahu, in line with the regional flexural trend of the island chain. The observed paleoshoreline depths for Kaua'i are in the range of depths predicted by our flexural correction model and are in agreement with those found by *Watts and ten Brink* [1989].

[26] Surrounding Ni'ihau, the slope of the bathymetry profiles above the slope break is 5° ± 3°, and below the slope break is 18° ± 3°. Two possible slope breaks are seen in the bathymetry west of Ni'ihau. These slope breaks are located on the end of ridges extending radially from the island (Figures 7 and 8). It is uncertain whether these ridges are remnants of highly mass wasted areas or whether they are volcanic rift zones. The best fitting plane through Ni'ihau's paleoshoreline, here called the P terrace (after the Pānī'au Volcanics, the shield building lavas of Ni'ihau [*Stearns*, 1947]), deepens from 820 m bsl south of the island to 1400 m bsl east of the island (Figures 7 and 8). The P terrace strikes north 3° east and dips 0.14° toward Kaua'i. The strike and dip of the P terrace suggests Ni'ihau has been tilted toward Kaua'i.

[27] Between the islands, two paleoshorelines are observed on the southern end of the Kaulakahi Channel, one at 1400 m bsl and the second at 870 m bsl (Figure 8). These slope breaks probably represent the overlap of Kaua'i's N terrace over Ni'ihau's P terrace. The paleoshoreline on the northern portion of the Kaulakahi Channel is ambiguous, with the N terrace identifiable halfway through the channel and the P terrace absent. However, the overlap of shorelines on the south side of the channel indicate that the east flank of Niihau is buried under the western flank of Kaua'i, a common feature for adjacent Hawaiian Islands [e.g., *Macdonald et al.*, 1983].

4. Discussion

4.1. Ni'ihau Residual Gravity

[28] The residual gravity high over the Kaulakahi Channel is interpreted to represent the solidified magma reservoir formed during Ni'ihau's shield stage, likely located under the island's center of volcanism. On the basis of the location of the residual gravity high, the center of Ni'ihau volcanism was as far as 13 km east of the island's eastern highlands. Exposed on the island's eastern cliff margin are hundreds of dikes, presumably marking a rift zone, supporting the interpretation of a center of volcanism east of the island [*Stearns*, 1947]. Combining the extent of Ni'ihau's paleoshoreline with the location of the Ni'ihau residual gravity anomaly, we infer that the subaerial portion of the Ni'ihau shield covered most of the

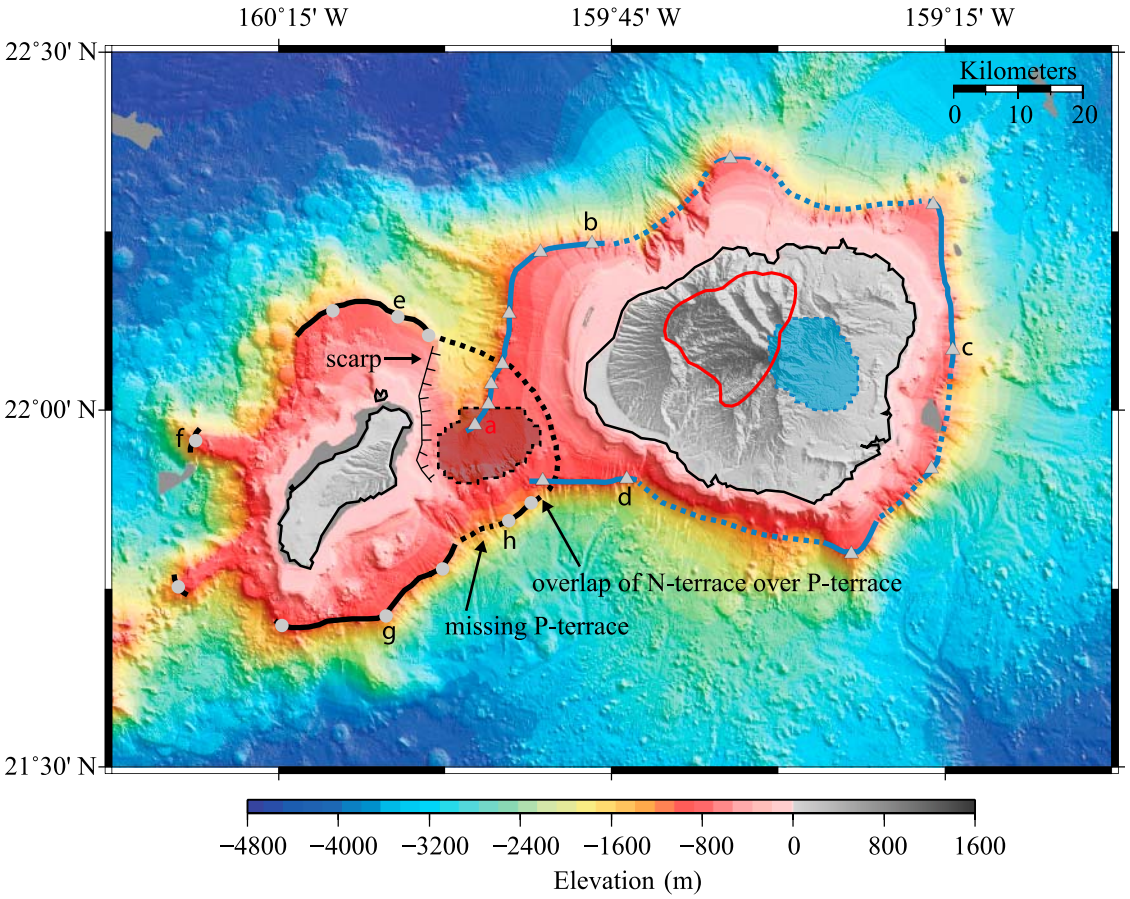

Figure 8. Qualitative reconstruction of the original extent of the Kaui'i and Ni'ihau subaerial shield volcanoes. The red line on Kaua'i outlines the boundaries of the inferred Waimea shield caldera, the Olokele volcanic member [*Macdonald et al.*, 1960]. Gray triangles (Kaua'i) and circles (Ni'ihau) mark identified paleoshoreline slope breaks. Solid thick lines trace paleoshorelines whereas short-dashed lines mark inferred paleoshorelines between identified slope breaks (circle and triangles) or around residual gravity highs. The Kaua'i paleoshoreline is shown in blue, Ni'ihau in black; the current shoreline is shown with a thin black line. Black and blue shaded colored regions are surface projections of the 3100 kg/m^3 isosurfaces, marking the presumed location of the volcanic summits. West of Ni'ihau slope breaks are located on the end of ridges extending radially from the island. These ridges may be island remnants after mass wasting or submarine rift zones. Letters adjacent to measured paleoshorelines locations refer to paleoshorelines profiles shown in Figure 7.

Kaulakahi Channel (Figure 8). Considering the lateral span of the gravity signal over the Kaulakahi Channel and the eastern extent of the P terrace, Ni'ihau's eastern coastline likely extended as far as 20 km eastward, twice the distance of previous estimates made by *Stearns* [1947] (10 km) and *Macdonald et al.* [1983] (8 km). The Ni'ihau shield was therefore axially asymmetric, with the volcanic summit lying east of the current geographic center of the island. We propose that the eastern portion of the island was likely removed through mass wasting or an eastern flank collapse.

[29] The dikes on Ni'ihau's eastern cliff margin strike 30°–50° northeast [*Stearns*, 1947], roughly parallel to the overall NW trend of the Ni'ihau residual gravity anomaly (Figure 5) and dikes on the western coast of Kaua'i (10°–40°; *Stearns* [1947]). The overall trend of these features from eastern Ni'ihau, through the Kaulakahi Channel, and inland to western Kaua'i, combined with the elongate trend of the residual gravity, supports previous interpretations of a long volcanic rift zone, the Mana ridge, passing through the present locations of both islands [*Krivoy et al.*, 1965; *Malahoff and Woollard*, 1966; *Holcomb et al.*, 1997]. Yet, whether this feature is an extension of the Ni'ihau volcanic center as proposed by *Krivoy et al.* [1965], a rift zone radiating away from Ni'ihau similar to Lō'ihi's rift system [*Walker*, 1990], a shared rift zone fed by either shield volcanoes [*Malahoff and Woollard*, 1966], or a separate and entirely unrelated feature, remains unresolved.

4.2. Kaua'i Residual Gravity

[30] The center of Kaua'i's residual gravity high is located over the Līhu'e Basin, offset 12 km SE from the center of the geologically mapped caldera (Figures 4a and 5). Gravity measurements in the caldera are limited because of terrain and access restrictions. It is possible that the residual high extends further to the west, but with the simplifying assumption that the Līhu'e Basin anomaly decreases at about the same rate to

the west as it does to the east and south, we infer that the peak gravity high is offset 8–12 km SE of the center of the mapped caldera. Whether a residual anomaly high exists in the unmeasured southern portion of the caldera is unknown. Any existing anomaly in this region would probably be only moderate or small in magnitude in order to decrease to the low residual gravity values seen along the southern coast of the island (Figure 5).

[31] The 8–12 km Kaua'i gravity-caldera displacement is the largest offset known for a hotspot island volcano. The next largest is Hualālai volcano on the island of Hawai'i, with a 7 km displacement from the nearest surface vents [*Kauahikaua et al.*, 2000]. Projecting the boundaries of Kaua'i's magma reservoir onto the regional map, given by our inversion model limited to the 3100 kg/m^3 isosurface, further illustrates this large offset (Figure 8). The large offset has important implications on the geological evolution of the island. Two possible scenarios for the offset are (1) the main shield-building magma reservoir is displaced away from the shield-stage (Olokele) caldera and (2) that the Olokele feature formed late in the shield stage and is not Kaua'i's long-term center of volcanism.

[32] Several complications arise if we assume the Olokele volcanics delineate the former shield-stage caldera as proposed by *Macdonald et al.* [1960]. Using depths to the top of the magma reservoir, given in Table 2, and the 8 km minimum lateral displacement between the residual gravity high and the center of the Olokele volcanics, the conduits bringing magma from the magma reservoir to the volcanic summit would have dipped only by 35° ± 5°, which is geologically unreasonable. Hawaiian shield volcano dikes typically dip 65°–85° [*Walker*, 1987]. The seismically inferred conduits of the active Hawaiian volcanoes dip nearly vertically [*Ryan*, 1988]. The size of the mapped caldera further complicates the classical interpretation. At 19 km long (NE-SW) and 16 km wide (NW-SE), it would be the largest caldera in the Hawaiian Islands [*Macdonald et al.*, 1960], with dimensions more than twice the size of the second largest caldera, located on East Moloka'i (7.7 km) [*Stearns and Macdonald*, 1947]. Large calderas are uncommon in both the Hawaiian Islands and other Pacific hotspot island chains, with the only large calderas (12–15 km) found on Hiva Oa (Marquesas Islands Chain) and the Gambier Islands (Pitcairn-Gambier Island Chain) [*Clouard et al.*, 2000], although the Gambier Islands caldera is poorly defined. The average diameter of calderas in French Polynesia, excluding Hiva Oa and the Gambier Islands, is 5 km [*Clouard et al.*, 2000]. Hawaiiain Island calderas, excluding East Moloka'i and the Olokele caldera, average 4 km in diameter, calculated from Ko'olau (4 km) [*Walker*, 1987], Moku'āweoweo (4 km) [*Macdonald et al.*, 1983], Lāna'i (5 km) [*Sherrod et al.*, 2007], Kahol'olawe (5 km) [*Walker*, 1990], West Maui (3 km) [*Sherrod et al.*, 2007], and Kīlauea (5 km) [*Macdonald et al.*, 1983]. The large size of the Olokele volcanic region does not preclude it from being formed by caldera subsidence, but the size is atypical for Pacific island calderas.

[33] *Macdonald et al.* [1960] defined the Olokele volcanics as the caldera region based on three field features: the greater thickness of individual lava flows within the caldera (6–22 m thick) compared to on the flanks of the volcano (1–5 m thick), the dip of the flows both inside (low dips, 1°–5°) versus outside (dipping radially away, 6°–12°) the caldera, and the location of interpreted fault scarps inferred to be the caldera boundary. However, on the basis of the *Macdonald et al.* [1960] data, we conclude that measurements of the dip of flows outside the mapped caldera are insufficient to confirm the original interpretation (being widespread and sparse), particularly along its presumed eastern boundary. The remaining observations used to define the caldera region support multiple processes. Any topographic depression where lavas pond, a caldera, eroded depression (e.g., Haleakalā Crater; *Macdonald et al.* [1983]), or a structural collapse, could produce these features.

[34] Alternatively, the currently mapped caldera is a late-collapse feature unrelated to the long-term center of Kaua'i shield volcanism. Instead, the original center of Kaua'i volcanism was located at the site of the residual gravity high, in the Līhu'e Basin. In this scenario, mass wasting created a large topographic depression in the originally interpreted Olokele caldera region, west of the true volcanic summit. This topographic depression was later filled with lava. The Līhu'e Basin center of volcanism then underwent a separate mass wasting event [*Sherrod et al.*, 2007]. This sequence of events is similar to the *Hazlett and Hyndman* [1996] cartoon model for the island's evolution. Thus, the large size of the Olokele Volcanic region reflects collapse and lava infilling rather than a former caldera. Smaller offsets of several kilometers between residual gravity highs and collapsed caldera-like features are seen in French Polynesia on Raivavae (Austral Islands), Morea, Tahaa, and Huahine (Society Islands) [*Clouard et al.*, 2000]. These offsets similarly have been interpreted as indicating that the collapsed feature is not linked to caldera subsidence but to mass wasting [*Clouard et al.*, 2000]. We found no indications in either the surface gravity mapping or the inverted density structure to support the hypothesis that Kaua'i was formed by two sequentially buttressed shield volcanoes, each having a separate magma supply system [*Holcomb et al.*, 1997].

4.3. The Relationship Between Kaua'i and Ni'ihau

[35] A 20 km long scarp in the bathymetry east of Ni'ihau and the 6 km long bathymetric section without a clear slope break in the southern portion of Kaulakahi Channel (Figure 8), further support a Ni'ihau eastern flank collapse (Figure 8). The presence of Kaua'i's paleoshoreline at shallower depths and overlapping Ni'ihau's suggests that Kaua'i's N terrace formed later and on top of the already submerged Ni'ihau P terrace. The growing Kaua'i shield tilted the Ni'ihau P terrace toward Kaua'i, resulting in the large west-to-east deepening of the P terrace (820 to 1400 m bsl) and helping submerge remaining features of eastern Ni'ihau. We can infer that Kaua'i and Ni'ihau were therefore not connected subaerially during the main period of either island's formation and that Ni'ihau's eastern flank collapse must have occurred prior to the formation of west Kaua'i's paleoshoreline and emplacement of Kaua'i's N terrace. The considerable overlap of K-Ar ages for shield-stage lavas on Ni'ihau, 5.0 ± 0.6 Ma [*Sherrod et al.*, 2007] and western Kaua'i, 4.7 ± 0.4 Ma [*McDougall*, 1979] suggests that the process that removed Ni'ihau's topographic summit probably occurred during a narrow time window, further supporting a flank collapse, which are common on Hawaiian volcanoes [*Moore et al.*, 1994].

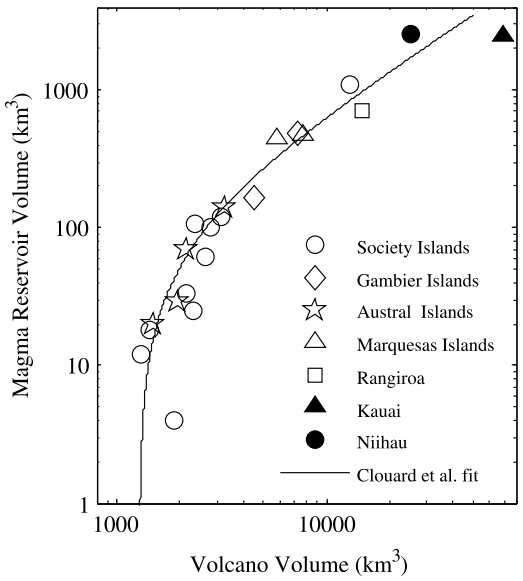

Figure 9. Logarithmic plot of magma reservoir volume versus volcano volume. The black line corresponds to a linear fit of volcanoes in French Polynesia, as presented by *Clouard et al.* [2000]. Kaua'i and Ni'ihau have comparable magma reservoir volumes but different volcano volume estimates [*Robinson and Eakins*, 2006]. The volume estimate of Ni'ihau volcano is a minimum because it does not include missing landslide material.

4.4. Characteristics of Magma Reservoirs

[36] The volume of the inferred magma reservoirs for Kaua'i and Ni'ihau (Table 2) are larger than those calculated using gravity data for other hotspot islands in French Polynesia [*Clouard et al.*, 2000]. The fixed density model used in French Polynesia [*Clouard et al.*, 2000] can be more directly compared to our variable density inversion, which allows densities as large as 3300 kg/m^3, by calculating the magma reservoir volumes for Kaua'i and Ni'ihau that results in an average density of 3100 kg/m^3, i.e., the fixed density used by *Clouard et al.* [2000]. The modeled magma reservoir for Kaua'i (2470 km^3) and Ni'ihau (2540 km^3) are in general agreement with the relationship between volcano volume and magma reservoir volume observed for French Polynesian volcanoes (Figure 9) [*Clouard et al.*, 2000]. Volcano volumes for Kaua'i (69,000 km^3) and Ni'ihau (25,300 km^3) were taken from the preliminary calculations of *Robinson and Eakins* [2006]. For both *Clouard et al.* [2000] and our comparison, the volcano volumes are based on the volume of material above abyssal seafloor and do not take into account compacted moat sediments or flexural deformation of the lithosphere. The roof depth of the modeled magma reservoirs for Kaua'i and Ni'ihau are similar to those found for magma reservoirs on Hawai'i [*Kauahikaua et al.*, 2000], varying from 2 to 5 km bsl.

[37] Kaua'i and Ni'ihau fall on opposing sides of the trend observed for French Polynesian volcanoes by *Clouard et al.* [2000] (Figure 9). The comparative size between Kaua'i's and Ni'ihau's magma reservoirs suggests that their volcano volumes should be similar, yet Kaua'i's volcano volume is more than twice that of Ni'ihau's. This inference is further support for a large volume of the Ni'ihau volcano collapsing to the east and being buried under younger Kaua'i volcanism, probably as landslide debris. This further supports our previous interpretation of an eastern Ni'ihau flank collapse. Such an event would imply that Kaua'i's volcano volume is smaller and Ni'ihau's volcano volume is larger than the current estimates. Resolving these volcano volume estimates would lead to closer agreement of Kaua'i and Ni'ihau with the trend observed for French Polynesian volcanoes (Figure 9).

5. Conclusion

[38] Analysis of on- and offshore gravity data reveals two prominent zones of positive residual gravity anomalies; one over the island of Kaua'i, and the other in the Kaulakahi Channel, between the islands of Kaua'i and Ni'ihau (Figure 5). The dimensions (20 × 20–30 km across) and magnitudes (maximum of 95–107 mGal) of the anomalies are comparable with those of other Hawaiian volcanoes. These anomalies are thought to be caused by buried bodies of high-density crust, most likely crystallized olivine cumulates in magma reservoirs (Figure 6). The depths (2–4.5 km bsl) of the magma reservoirs for Kaua'i and Ni'ihau are comparable to those found beneath other hotspot islands in French Polynesia [*Clouard et al.*, 2000] and Hawai'i [*Kauahikaua et al.*, 2000]. The volumes (2470–2540 km^3) of the magma reservoirs for Kaua'i and Ni'ihau are larger than those observed in French Polynesia [*Clouard et al.*, 2000] but generally agree with the relationship between volcano volume and magma reservoir volume previously observed by *Clouard et al.* [2000].

[39] Kaua'i's gravity anomaly, attributed to the magma reservoir of the Waimea shield volcano, is offset 8–12 km east of Kaua'i's geologically mapped caldera (Figure 8) (defined by the Olokele volcanics). We interpret this structural depression to be a late feature formed by mass wasting and later infilled with lava rather than the volcanic summit or caldera. Instead, the summit of the Waimea shield volcano was located 12 km to the east, over the residual gravity anomaly in the Līhu'e Basin. The summit of the volcano was likely removed by extensive mass wasting and/or erosion.

[40] The location of the Ni'ihau residual gravity anomaly (Figure 5), in the Kaulakahi Channel, indicates that the eastern boundary of Ni'ihau was ~20 km east of its present location (Figure 8), twice the distance of previous estimates. We identified bathymetric slope breaks around both islands and attributed these to the shield-stage paleoshorelines (Figures 7 and 8). Combining the locations of the residual gravity highs, the extent of the paleoshorelines, and potassium-argon dating of shield-stage lavas, we conclude that the Kaua'i and Ni'ihau volcanoes were not connected subaerially during their respective shield stages and that Ni'ihau's topographic summit was probably removed rapidly by an eastern flank collapse (Figure 8). Continued constructional volcanism on western Kaua'i likely covered the submerged remains of eastern Ni'ihau.

Appendix A: Three-Dimensional Geophysical Inversion Theory

[41] We performed 3-D inversion using the GRAV3D program library [*GRAV3D*, 2007]; its methodology is

discussed briefly below, following the study of *Li and Oldenburg* [1998].

[42] The vertical component of the gravity field produced by the density $\rho(x, y, z)$ at location $\vec{r}_i$ is

$$F_z(\vec{r}_i) = \gamma \int_V \rho(\vec{r}) \frac{z - z_i}{|\vec{r} - \vec{r}_i|^3} dv, \quad \text{(A1)}$$

where $\vec{r}$ is the source location, $\vec{r}_i$ is the observation location, V is the volume of the model domain, and γ is Newton's gravitational constant. The above equation can be rewritten in matrix notation in terms of a kernel function **G**,

$$\mathbf{G}\vec{\rho} = \vec{d}, \quad \text{(A2)}$$

where $\vec{d} = (d_1, \ldots d_N)$ contains the N observations (the residual gravity) and $\vec{\rho} = (\rho_1, \ldots \rho_M)$ contains the M density values of the model volume. In order to recover the density distribution from the observed residual gravity data $F_z(\vec{r}_i)$, we define the data misfit using the two-norm measure

$$\phi_d = \left\| E_d(\vec{d} - \vec{d}^{obs}) \right\|_2^2, \quad \text{(A3)}$$

where $\vec{d}^{obs} = (F_{z1}, \ldots, F_{zN})^T$ is the observed data, and $\vec{d}$ is the predicted data. Defining $E_d = diag\{1/\sigma_1, \ldots, 1/\sigma_N\}$ and σ_i as an estimate of uncertainty of the ith observation, makes ϕ_d a χ^2 random variable with N degrees of freedom. An acceptable model is one where the misfit ϕ_d is approximately equal to the number of observations N. Because of the nonuniqueness of solutions to potential field data, there are infinitely many density distributions that will reproduce the known. GRAV3D defines a generalized model objective function requiring that it be close to a reference model ρ_0 and that it produce a smooth model in three spatial directions. The model objective function is given by

$$\begin{aligned}\phi_m(\rho) = {} & \alpha_s \int_V w_s w^2(\vec{r})(\rho - \rho_0)^2 dv + \alpha_x \int_V w_x \left(\frac{\partial w(z)(\rho - \rho_0)}{\partial x} \right)^2 dv \\ & + \alpha_y \int_V w_y \left(\frac{\partial w(z)(\rho - \rho)}{\partial y} \right)^2 dv \\ & + \alpha_z \int_V w_z \left(\frac{\partial w(z)(\rho - \rho_0)}{\partial z} \right)^2 dv \end{aligned} \quad \text{(A4)}$$

or similarly,

$$\phi_m(\vec{\rho}) = \|E_m(\vec{\rho} - \vec{\rho}_0)\|_2^2, \quad \text{(A5)}$$

where w_s, w_x, w_y, and w_z are spatially dependent weighting functions, α_s, α_x, α_y, and α_z are coefficients that define the relative importance and resolution of different terms in the objective function, and E_m is a function incorporating both sets of aforementioned terms. Increasing the ratio α_j/α_s, where $j = x, y, z$, causes the recovered model to be smoother in the j direction. The kernel function for the observed surface gravity G_{ij} decays with inverse distance squared and as a result, any model that minimizes $\|\rho - \rho_0\|_2^2$ subject to fitting the data will produce a density distribution that is concentrated near the surface. GRAV3D therefore implements a weighting function $w(\vec{r})$ that compensates for the kernel's natural decay by giving cells at different depths equal probability of a being incorporated into the solution with a nonzero value. We use a normalized weighting function that varies with depth and is generalized by

$$w(\vec{r}_j) = \left[\frac{1}{\Delta z_j} \int_{\Delta zj} \frac{dv}{(z + z_0)^2} \right]^{\frac{1}{2}}, \quad j = 1, \ldots, M \quad \text{(A6)}$$

where $\vec{r}_j$ is the distance between the jth cell and an observation point Δz_j is its thickness and z is its depth below the observation point. Decreasing z_0 will cause the depth weighting function to be maximized.

[43] The inverse problem is solved by minimizing

$$\phi(\rho) = \phi_d + \mu\phi_m \quad \text{(A7)}$$

where μ is a regularization that controls the importance of the model objective function (ϕ_m) relative to the data misfit (ϕ_d). The minimization is solved subject to upper and lower bound constraints of the solution density, using a primal logarithmic barrier method with the conjugate gradient technique.

[44] **Acknowledgments.** We thank F. Duennebier, P. Wessel, O. Neill, A. Aryal, M. Chandler, B. Kastl, and C. Parcheta for helpful reviews of an early version of this manuscript and J. Kauahikaua and V. Clouard for reviews of the final publication. Our appreciation goes out to J. Sinton, B. Taylor, and D. Clague for insightful comments throughout the course of the project. C. Blay provided us with invaluable local knowledge of Kaua'i and accommodation while performing the land gravity survey. We were assisted in all things GPS related by J. Foster. A special thank you to M. Barbee and S.-S. Kim for assistance with data compilation. Land access on Kauai was provided by R. Rice of Kipu Ranch, D. Hinazumi of Grove Farm Company Inc., R. Licona and the Department of Hawaiian Homelands, and G. Kawakami and the Division of Forestry and Wildlife Kauai District. T. McGovern of the University of Hawai'i Marine Center assisted us in accessing available marine gravity data. B. Applegate and the captain and crew of the *R/V Kilo Moana* cruise KM0718 helped make the marine survey possible. This work was supported by NSF grant EAR05-10482 to M.G. and G.I., and the University of Hawaii Foundation's Harold T. Stearns Fellowship to A.F. This is SOEST contribution 7904.

References

Blakely, R. J. (1996), *Potential Theory in Gravity and Magnetic Applications*, 441 pp., Cambridge University Press, New York.

Bottinga, Y., and D. F. Weill (1970), Densities of liquid silicate systems calculated from partial molar volumes of oxide components, *Am. J. Sci.*, *269*, 169–182.

Cashman, K. V., and J. P. Kauahikaua (1997), Reevaluation of vesicle distributions in basaltic lava flows, *Geology*, *25*, 419–422.

Clague, D. A. (1987), Hawaiian xenolith populations, magma supply rates and development of magma chambers, *Bull. Volcanol.*, *49*, 577–587.

Clague, D. A. (1990), Kauai, in *Volcanoes of North America*, edited by C. A. Wood and J. Kienle, Cambridge University Press, New York.

Clague, D. A., and P. R. Denlinger (1994), Role of olivine cumulates in destabilizing the flanks of Hawaiian volcanoes, *Bull. Volcanol.*, *56*, 425–434.

Clouard, V., A. Bonneville, and H. G. Barsczus (2000), Size and depth of ancient magma reservoirs under atolls and islands of French Polynesia using gravity data, *J. Geophys. Res.*, *105*, 8173–8191.

Dana, J. D. (1890), *Characteristics of Volcanoes*, 312 pp., Dodd, Mead and Co., New York.

Garcia, M. O., L. Swinnard, D. Weis, A. R. Greene, T. Tagami, H. Sano, and C. E. Gandy (2010), Petrology, geochemistry and geochronology of Kaua`i lavas over 4.5 Myr: Implications for the origin of rejuvenated volcanism and the evolution of the Hawaiian plume, *J. Petrol.*, *51*, 1–34, doi:10.1093/petrology/egq027.

GRAV3D (2007), A program library for forward modeling and inversion of gravity data over 3D structures, *Joint/Cooperative Inversion of Geophysical Data, Ver. 3.0*, UBC Geophysical Inversion Facility, Univ. British Columbia, Vancouver.

Holcomb, R. T., P. W. Reiners, B. K. Nelson, and N. E. Sawyer (1997), Evidence for two shield volcanoes exposed on the island of Kauai, Hawaii, *Geology*, *25*, 811–814.

Hazlett, R. W., and D. W. Hyndman (1996), *Roadside Geology of Hawaii*, 304 pp., Mountain Press Publishing Co., Mont.

Kauahikaua, J., T. Hildenbrand, and M. Webring (2000), Deep magmatic structures of Hawaiian volcanoes, imaged by three-dimensional gravity models, *Geology*, *28*, 883–886.

Kinoshita, W. T., H. L. Krivoy, D. R. Mabey and R. R. Macdonald (1963), Gravity survey of the island of Hawaii, *U.S. Geo. Surv. Prof. Paper 475-C*, 114–116, U.S. Government Printing Office, Washington.

Krivoy, H. L. (1965), A gravity survey of the island of Niihau, Hawaii, *Pac. Sci.*, *19*, 359–360.

Krivoy, H. L., and J. P. Eaton (1961), Preliminary gravity survey of Kilauea volcano, Hawaii, *U.S. Geo. Surv. Prof. Paper P 0424-D*, U.S. Government Printing Office, Washington.

Krivoy, H. L., B. Melville, and E. E. Moe (1965), A reconnaissance gravity survey of the island of Kauai, Hawaii, *Pac. Sci.*, *19*, 354–358.

Li, Y., and D. W. Oldenburg (1998), 3-D inversion of gravity data, *Geophysics*, *63*, 109–119.

Maaloe, S., D. James, P. Smedley, S. Peterson, and L. B. Garmann (1992), The Koloa Volcanic Suite of Kauai, Hawaii, *J. Pterol.*, *33*, 1–24.

Macdonald, G. A., D. A. Davis, and D. C. Cox (1960), Geology and ground-water resources of the island of Kauai, Hawaii, *Hawaii Division of Hydrography, Bulletin*, *13*, 1–212.

Macdonald, G. A., A. T. Abbott, and F. L. Peterson (1983), *Volcanoes in the Sea*, 517 pp., University of Hawaii Press, Honolulu, HI.

Malahoff, A., and G. P. Woollard (1966), Magnetic surveys over the Hawaiian islands and their geologic implications, *Pac. Sci.*, *20*, 265–311.

Mark, R. K., and J. G. Moore (1987), Slopes of the Hawaiian ridges, *U.S. Geo. Surv. Prof. Paper 1350*, 101–107, U.S. Government Printing Office, Washington.

McDougall, I. (1979), Age of shield-building volcanism of Kauai and linear migration of volcanism in the Hawaiian Island Chain, *Earth Planet. Sci. Lett.*, *46*, 31–42.

McNutt, M. K., and L. Shure (1986), Estimating the compensation depth of the Hawaiian swell with linear filters, *J. Geophys. Res.*, *91*, 13,915–13,923.

Moore, J. G. (1987), Subsidence of the Hawaiian ridge, *U.S. Geo. Surv. Prof. Paper 1350*, 85–100, U.S. Government Printing Office, Washington.

Moore, J. G., W. R. Normak, and R. T. Holcomb (1994), Giant Hawaiian landslides, *Annu. Rev. Earth Planet Sci.*, *22*, 119–144.

Mukhopadhyay, S., J. C. Lassiter, K. A. Farley, and S. W. Bogue (2003), Geochemistry of Kauai shield-stage lavas: implications for the chemical evolution of the Hawaiian plume, *Geochem. Geophys. Geosyst.*, *4*(1), 1009, doi:10.1029/2002GC000342.

Parker, R. L. (1973), The rapid calculation of potential anomalies, *Geophys. J. R. Astron. Soc.*, *51*, 447–455.

Ponce, D. A., T. G. Hildenbrand, J. Kauahikaua, and C. H. Degnan (1994), Major features on maps of shipborne gravity, magnetic and bathymetric data of the offshore Hawaiian islands collected during the GLORIA program, *Eos Trans. AGU*, *75*.

Prince, R. A., and D. W. Forsyth (1984), A simple objective method for minimizing crossover errors in marine gravity data, *Geophysics*, *49*, 1070–1083.

Reiners, P. W., B. K. Nelson, and S. K. Izuka (1999), Structural and petrologic evolution of the Lihu'e Basin and eastern Kauai, Hawaii, *Geol. Soc. Am. Bull.*, *111*, 674–685.

Robinson, J. E., and B. W. Eakins (2006), Calculated volumes of individual shield volcanoes at the young end of the Hawaiian Ridge, *J. Volcanol. Geotherm. Res.*, *151*, 309–317, doi:10.1016/j.jvolgeores.2005.07.033.

Ryan, M. P. (1988), The mechanics and three-dimensional internal structure of active magmatic systems: Kilauea Volcano, Hawaii, *J. Geophys. Res.*, *93*, 4213–4248.

Smith, W. H. F., and D. T. Sandwell (1997), Global seafloor topography from satellite altimetry and ship depth soundings, *Science*, *277*, 1957–1962.

Schmidt, R., and H. U. Schmincke (2000), Seamounts and island building, in *Encyclopedia of Volcanoes*, edited by H. Sigurdsson, pp. 383–402, Academic Press, London.

Sherrod, D. R., J. M. Sinton, S. E. Watkins, and K. M. Brunt (2007), Geologic map of the state of Hawaii, *USGS Open File Rep. 2007-1089*, 85 pp.

Stearns, H. T. (1946), Geology of the Hawaiian Islands, *Hawaii Division of Hydrography, Bull.*, *8*, 106 pp.

Stearns, H. T. (1947), Geology and ground-water resources of the island of Niihau, Hawaii, *Hawaii Division of Hydrography, Bull.*, *12*, 1–37.

Stearns, H. T., and G. A. Macdonald (1947), Geology and ground-water resources of the island of Molokai, Hawaii, *Hawaii Division of Hydrography, Bull.*, *11*, 113 pp.

Strange, W. E., G. P. Woollard, and J. C. Rose (1965), An analysis of the gravity field over the Hawaiian Islands in terms of crustal structure, *Pac. Sci.*, *19*, 381–389.

Turcotte, D. L., and G. Schubert (2002), *Geodynamics*, 2nd ed., Cambridge University Press, New York.

Walcott, R. I. (1970), Flexure of the lithosphere at the Hawaiian islands, *Tectonophysics*, *9*, 435–446.

Walker, G. P. L. (1990), Geology and volcanology of the Hawaiian Islands, *Pac.Sci.*, *44*, 315–347.

Walker, G. P. L. (1987), The dike complex of Koolau Volcano, Oahu: Internal structure of the Hawaiian rift zone, *USGS Prof. Paper 1350*, 961–993.

Watts, A. B., and J. R. Cochran (1974), Gravity anomalies and flexure of the lithosphere along the Hawaiian-Emperor seamount chain, *Geophys. J. R. Astron. Soc.*, *38*, 119–141.

Watts, A. B., and U. S. ten Brink (1989), Crustal structure, flexure and subsidence history of the Hawaiian islands, *J. Geophys. Res.*, *94*, 10,473–10,500.

Wessel, P. (1993), A reexamination of the flexural deformation beneath the Hawaiian islands, *J. Geophys. Res.*, *98*, 12,177–12,190.

Wessel, P., and B. K. Keating (1994), Temporal variations of flexural deformation in Hawaii, *J. Geophys. Res.*, *99*, 2747–2756.

Wessel, P., and W. H. F. Smith (1991), Free software helps map and display data, *EOS Trans. AGU*, *72*, 441.

Zucca, J. J., D. P. Hill, and R. L. Kovach (1982), Crustal structure of Mauna Loa volcano, Hawaii, from seismic refraction and gravity data, *Bull. Seis. Soc. Am.*, *72*, 1535–1550.

A. F. Flinders, M. O. Garcia, and G. Ito, Department of Geology and Geophysics, University of Hawai'i, 1680 East-West Road, Honolulu, HI 96822, USA. (gito@hawaii.edu)